

GLINKX: A SCALABLE UNIFIED FRAMEWORK FOR HOMOPHILOUS AND HETEROPHILOUS GRAPHS

Marios Papachristou*
Cornell University
papachristoumarios@gmail.com

Rishab Goel
Twitter Inc.
rgoel@twitter.com

Frank Portman
Twitter Inc.
fportman@twitter.com

Matthew Miller
Twitter Inc.
mmiller@twitter.com

Rong Jin
Twitter Inc.
rj@twitter.com

ABSTRACT

In graph learning, there have been two predominant inductive biases regarding graph-inspired architectures: On the one hand, higher-order interactions and message passing work well on homophilous graphs and are leveraged by GCNs and GATs. Such architectures, however, cannot easily scale to large real-world graphs. On the other hand, shallow (or node-level) models using ego features and adjacency embeddings work well in heterophilous graphs. In this work, we propose a novel scalable shallow method – GLINKX – that can work both on homophilous and heterophilous graphs. GLINKX leverages (i) novel monophilous label propagations (ii) ego/node features, (iii) knowledge graph embeddings as positional embeddings, (iv) node-level training, and (v) low-dimensional message passing. Formally, we prove novel error bounds and justify the components of GLINKX. Experimentally, we show its effectiveness on several homophilous and heterophilous datasets.

1 INTRODUCTION

In recent years, graph learning methods have emerged with a strong performance for various ML tasks. Graph ML methods leverage the topology of graphs underlying the data (Battaglia et al., 2018) to improve their performance. Two very important design options for proposing graph ML based architectures in the context of *node classification* are related to whether the data is *homophilous* or *heterophilous*.

For homophilous data – where neighboring nodes share similar labels (McPherson et al., 2001; Altenburger & Ugander, 2018a) – Graph Neural Network (GNN)-based methods are able to achieve high accuracy. Specifically, a broad subclass successful GNNs are Graph Convolutional Networks (GCNs) (e.g., GCN, GAT, etc.) (Kipf & Welling, 2016; Veličković et al., 2017; Zhu et al., 2020). In the GCN paradigm, *message passing* and *higher-order interactions* help node classification tasks in the homophilous setting since such inductive biases tend to bring the learned representations of linked nodes close to each other. However, GCN-based architectures suffer from *scalability issues*. Performing (higher-order) propagations during the training stage are hard to scale in large graphs because the number of nodes grows exponentially with the increase of the filter receptive field. Thus, for practical purposes, GCN-based methods require *node sampling*, substantially increasing their training time. For this reason, architectures (Huang et al., 2020; Zhang et al., 2022b; Sun et al., 2021; Maurya et al., 2021; Rossi et al., 2020) that leverage propagations outside of the training loop (as a preprocessing step) have shown promising results in terms of scaling to large graphs.

In *heterophilous* datasets (Rogers et al., 2014), the nodes that are connected tend to have different labels. Currently, many works that address heterophily can be classified into two categories concerning scale. On the one hand, recent successful architectures (in terms of accuracy) (Jin et al., 2022a; Di Giovanni et al., 2022; Zheng et al., 2022b; Luan et al., 2021; Chien et al., 2020; Lei et al., 2022) that address heterophily resemble GCNs in terms of design and thus suffer from the same scalability

*Work done while interning at Twitter.

issues. On the other hand, *shallow or node-level models* (see, e.g., (Lim et al., 2021; Zhong et al., 2022)), i.e., models that are treating graph data as tabular data and do not involve propagations during training, has shown a lot of promise for large heterophilous graphs. In (Lim et al., 2021), it is shown that combining ego embeddings (node features) and adjacency embeddings works in the heterophilous setting. One element that LINKX exploits via the adjacency embeddings is monophily (Altenburger & Ugander, 2018a;b), namely the similarity of the labels of a node’s neighbors. However, their design is still impractical in real-world data since the method (LINKX) is *not* inductive (see Section 2), and embedding the adjacency matrix directly requires many parameters in a model. In LINKX, the adjacency embedding of a node can alternatively be thought of as a *positional embedding* (PE) of the node in the graph, and recent developments (Kim et al., 2022; Dwivedi et al., 2021; Lim et al., 2021) have shown the importance of PEs in both homophilous and heterophilous settings. However, most of these works suggest PE parametrizations that are difficult to compute in large-scale settings. We argue that PEs can be obtained in a scalable manner by utilizing *knowledge graph embeddings*, which, according to prior work, can (El-Kishky et al., 2022; Lerer et al., 2019; Bordes et al., 2013; Yang et al., 2014) be trained in very large networks.

Goal & Contribution: In this work, we develop a scalable method for node classification that: (i) works both on homophilous and heterophilous graphs, (ii) is *simpler and faster* than conventional message passing networks (by avoiding the neighbor sampling and message passing overhead during training), and (iii) can work in both a *transductive* and an *inductive*¹ setting. For a method to be scalable, we argue that it should: (i) run models on node-scale (thus leveraging i.i.d. minibatching), (ii) avoid doing message passing during training and do it a constant number of times before training, and (iii) transmit small messages along the edges. Our proposed method – GLINKX (see Section 3) – combines all the above desiderata. GLINKX has three components: (i) ego embeddings², (ii) PEs inspired by architectures suited for heterophilous settings, and (iii) *scalable* 2nd-hop-neighborhood propagations inspired by architectures suited for homophilous settings (Section 2.5). We provide novel theoretical error bounds and justify components of our method (Section 3.4). Finally, we evaluate GLINKX’s empirical effectiveness on several homophilous and heterophilous datasets (Section 4).

2 PRELIMINARIES

2.1 NOTATION

We denote scalars with lower-case, vectors with bold lower-case letters, and matrices with bold upper-case. We consider a directed graph $G = G(V, E)$ with vertex set V with $|V| = n$ nodes, and edge set E with $|E| = m$ edges, and adjacency matrix \mathbf{A} . $\mathbf{X} \in \mathbb{R}^{n \times d_x}$ represents the d_x -dimensional features and $\mathbf{P} \in \mathbb{R}^{n \times d_p}$ represent the d_p -dimensional PE matrix. A node i has a feature vector $\mathbf{x}_i \in \mathbb{R}^{d_x}$ and a positional embedding $\mathbf{p}_i \in \mathbb{R}^{d_p}$ and belongs to a class $y_i \in \{1, \dots, c\}$. The training set is denoted by $G_{\text{train}}(V_{\text{train}}, E_{\text{train}})$, the validation set by $G_{\text{valid}}(V_{\text{valid}}, E_{\text{valid}})$, and test set by $G_{\text{test}}(V_{\text{test}}, E_{\text{test}})$. $\mathbb{I}\{\cdot\}$ is the indicator function. Γ_c is the c -dimensional simplex.

2.2 GRAPH CONVOLUTIONAL NEURAL NETWORKS

In homophilous datasets, GCN-based methods have been used for node classification. GCNs (Kipf & Welling, 2016) utilize feature propagations together with non-linearities to produce node embeddings. Specifically, a GCN consists of multiple layers where each layer i collects i -th hop information from the nodes through propagations and forwards this information to the $i + 1$ -th layer. More specifically, if G has a symmetrically-normalized adjacency matrix \mathbf{A}'_{sym} (with self-loops) (ignoring the directionality of edges), then a GCN layer has the form

$$\mathbf{H}^{(0)} = \mathbf{X}, \mathbf{H}^{(i+1)} = \sigma \left(\mathbf{A}'_{\text{sym}} \mathbf{H}^{(i)} \mathbf{W}^{(i)} \right) \forall i \in [L], \mathbf{Y} = \text{softmax} \left(\mathbf{H}^{(L)} \right).$$

Here $\mathbf{H}^{(i)}$ is the embedding from the previous layer, $\mathbf{W}^{(i)}$ is a learnable projection matrix and $\sigma(\cdot)$ is a non-linearity (e.g. ReLU, sigmoid, etc.).

¹For this paper, we operate in the *transductive setting*. See App. B for the inductive setting.

²We use ego embeddings and node features interchangeably.

Algorithm 1 GLINKX Algorithm**Input:** Graph $G(V, E)$ with train set $V_{\text{train}} \subseteq V$, node features \mathbf{X} , labels \mathbf{Y} **Output:** Node Label Predictions $\mathbf{Y}_{\text{final}}$ **1st Stage (KGEs).** Pre-train knowledge graph embeddings \mathbf{P} with Pytorch Biggraph.**2nd Stage (MLaP).** Propagate labels and predict neighbor distribution

1. **MLaP Forward:** Calculate the distribution of each training node’s neighbors, i.e.

$$\hat{\mathbf{y}}_i = \frac{\sum_{j \in V_{\text{train}}: (j,i) \in E_{\text{train}}} \mathbf{y}_j}{|\{j \in V_{\text{train}}: (j,i) \in E_{\text{train}}\}|} \text{ for all } i \in V_{\text{train}}$$

2. **Learn distribution of a node’s neighbors:**

- (a) For each epoch, calculate $\tilde{\mathbf{y}}_i = f_1(\mathbf{x}_i, \mathbf{p}_i; \boldsymbol{\theta}_1)$ for $i \in V_{\text{train}}$

- (b) Update the parameters s.t. the negative cross-entropy

$$\mathcal{L}_{\text{CE},1}(\boldsymbol{\theta}_1) = \sum_{i \in V_{\text{train}}} \text{CE}(\hat{\mathbf{y}}_i, \tilde{\mathbf{y}}_i; \boldsymbol{\theta}_1) \text{ is maximized in order to bring } \tilde{\mathbf{y}}_i \text{ statistically close to } \hat{\mathbf{y}}_i.$$

- (c) Let $\boldsymbol{\theta}_1^*$ be the parameters at the end of the training that correspond to the epoch with the best validation accuracy.

3. **MLaP Backward:** Calculate $\mathbf{y}'_i = \frac{\sum_{j \in V: (i,j) \in E} \tilde{\mathbf{y}}_j}{|\{j \in V: (i,j) \in E\}|}$ for all $i \in V_{\text{train}}$, where

$$\tilde{\mathbf{y}}_j = f_1(\mathbf{x}_j, \mathbf{p}_j; \boldsymbol{\theta}_1^*).$$

3rd Stage (Final Model). Predicting node’s own label distribution:

1. For each epoch, calculate $y_{\text{final},i} = f_2(\mathbf{x}_i, \mathbf{p}_i, \mathbf{y}'_i; \boldsymbol{\theta}_2)$.

2. Update the parameters s.t. the negative cross-entropy

$$\mathcal{L}_{\text{CE},2}(\boldsymbol{\theta}_2) = \sum_{i \in V_{\text{train}}} \text{CE}(y_i, y_{\text{final},i}; \boldsymbol{\theta}_2) \text{ is maximized.}$$

Return $\mathbf{Y}_{\text{final}}$

2.3 LINKX

In heterophilous datasets, the simple method of LINKX has been shown to perform well. LINKX combines two components – MLP on the node features \mathbf{X} and LINK regression (Altenburger & Ugander, 2018a) on the adjacency matrix – as follows:

$$\mathbf{H}_X = \text{MLP}_X(\mathbf{X}), \mathbf{H}_A = \text{MLP}_A(\mathbf{A}), \mathbf{Y} = \text{ResNet}(\mathbf{H}_X, \mathbf{H}_A).$$

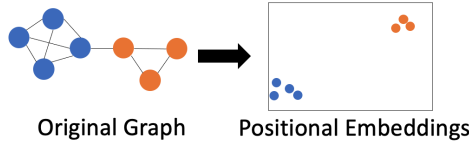
2.4 NODE CLASSIFICATION

In node classification problems on graphs, we have a model $f(\mathbf{X}, \mathbf{Y}_{\text{train}}, \mathbf{A}; \boldsymbol{\theta})$ that takes as an input the node features \mathbf{X} , the training labels $\mathbf{Y}_{\text{train}}$ and the graph topology \mathbf{A} and produces a prediction for each node i of G , which corresponds to the probability that a given node belongs to any of c classes (with the sum of such probabilities being one). The model is trained with back-propagation. Once trained, the model can be used for the prediction of labels of nodes in the test set.

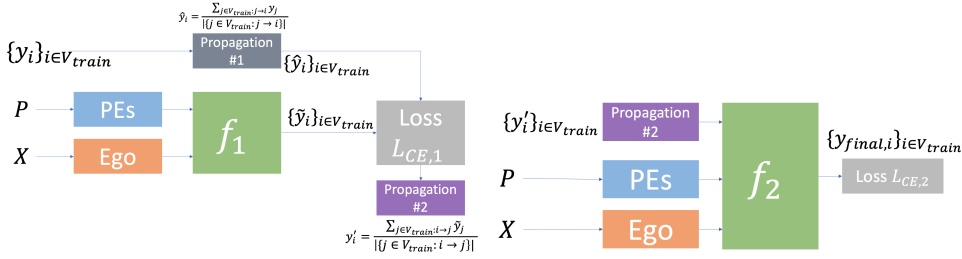
There are two training regimes: *transductive* and *inductive*. In the transductive training regime, we have full knowledge of the graph topology (for the train, test, and validation sets) and the node features, and the task is to predict the labels of the validation and test set. In the inductive regime, only the graph induced by V_{train} is known at the time of training, and then the full graph is revealed for prediction on the validation and test sets. In real-world scenarios, such as online social networks, the dynamic nature of problems makes the inductive regime particularly useful.

2.5 HOMOPHILY, HETEROHILY & MONOPHILY

Homophily and Heterophily: There are various measures of homophily in the GNN literature like node homophily and edge homophily Lim et al. (2021). Intuitively, homophily in a graph implies that nodes with similar labels are connected. GNN-based approaches like GCN, GAT, etc., leverage this property to improve the node classification performance. Alternatively, if a graph has low homophily – namely, nodes that connect tend to have different labels – it is said to be *heterophilous*. In other words, a graph is heterophilous if neighboring nodes do not share similar labels.



(a) 1st Stage



(b) 2nd Stage

(c) 3rd Stage

Figure 1: Block Diagrams of GLINKX stages.

Monophily: Generally, we define a graph to be monophilous if the label of a node is similar to that of its neighbors’ neighbors³. Etymologically, the word “monophily” is derived from the Greek words “*monos*” (unique) and “*philos*” (friend), which in our context means that a node – regardless of its label – has neighbors of primarily one label. In the context of a directed graph, monophily can be thought of as a structure that resembles Fig. 2(a) where similar nodes (in this case, three green nodes connected to a yellow node) are connected to a node with a different label.

We argue that encoding monophily into a model **can be helpful for both heterophilous and homophilous graphs (see Figs. 3(b) and 3(c)), which is one of the main motivators behind our work.** In homophilous graphs, monophily will fundamentally encode the 2nd-hop neighbor’s label information, and since in such graphs, neighboring nodes have similar labels, it can provide a helpful signal for node classification. In heterophily, neighboring nodes have different labels, but the 2nd-hop neighbors may share the same label, providing helpful information for node classification. Monophily is effective for heterophilous graphs (Lim et al., 2021). Therefore, an approach encoding monophily has an advantage over methods designed specifically for homophilous and heterophilous graphs, especially when varying levels of homophily can exist between different sub-regions in the same graph (see Section 3.3). It may also not be apparent if the (sub-)graph is purely homophilous/heterophilous (since these are not binary constructs), which makes a unified architecture that can leverage graph information for both settings all the more important.

3 METHOD

3.1 COMPONENTS & MOTIVATION

The desiderata we laid down on Section 1 can be realized by three components: (i) PEs, (ii) ego embeddings, and (iii) label propagations that encode monophily. More specifically, ego embeddings and PEs are used as primary features, which have been shown to work for both homophilous and heterophilous graphs for the models we end up training. Finally, the propagation step is used to encode monophily to provide additional information to our final prediction.

Positional Embeddings: We use PEs to provide our model information about the position of each node and hypothesize that PEs are an important piece of information in the context of large-scale node classification. PEs have been used to help discriminate isomorphic graph (sub)-structures (Kim et al., 2022; Dwivedi et al., 2021; Srinivasan & Ribeiro, 2019). This is useful for both homophily (Kim et al., 2022; Dwivedi et al., 2021) and heterophily (Lim et al., 2021) because isomorphic (sub)-structures can exist in both the settings. In the homophilous case, adding positional information can help

³A similar definition of monophily has appeared in (Altenburger & Ugander, 2018a), whereby many nodes have extreme preferences for connecting to a certain class.

distinguish nodes that have the same neighborhood but distinct position (Dwivedi et al., 2021; Morris et al., 2019; Xu et al., 2019), circumventing the need to do higher-order propagations (Dwivedi et al., 2021; Li et al., 2019; Bresson & Laurent, 2017) which are prone to over-squashing (Alon & Yahav, 2021). In heterophily, structural similarity among nodes is important for classification, as in the case of LINKX – where adjacency embedding can be considered a PE. However, in large graphs, using adjacency embeddings or Laplacian eigenvectors (as methods such as (Kim et al., 2022) suggest) can be a computational bottleneck and may be infeasible.

In this work, we leverage *knowledge graph embeddings* (KGEs) to encode positional information about the nodes, and embed the graph. Using KGEs has two benefits: Firstly, KGEs can be trained quickly for large graphs. This is because KGEs compress the adjacency matrix into a fixed-sized embedding, and adjacency matrices have been shown to be effective in heterophilous cases. Further, KGEs are lower-dimensional than the adjacency matrix (e.g., $d_P \sim 10^2$), allowing for faster training and inference times. Secondly, KGEs can be pre-trained efficiently on such graphs (Lerer et al., 2019) and can be used off-the-shelf for other downstream tasks, including node classification (El-Kishky et al., 2022)⁴. So, in the 1st Stage of our methods in Alg. 1 (Fig. 1(a)) we train KGEs model on the available graph structure. Here, we fix this positional encoding once they are pre-trained for downstream usage. Finally, we note that this step is transductive but we can easily make it inductive (El-Kishky et al., 2022; Albooyeh et al., 2020).

Ego Embeddings: We get ego embeddings from the node features. Such embeddings have been used in homophilous and heterophilous settings (Lim et al., 2021; Zhu et al., 2020). Node embeddings are useful for tasks where the graph structure provides little/no information about the task.

Monophilous Label Propagations: We now propose a novel monophily (refer Section 2.5) inspired label propagation which we refer to as Monophilous Label Propagation (MLaP). MLaP has the advantage that we can use it both for homophilous and heterophilous graphs or in a scenario with varying levels of graph homophily (see Section 3.3) as it encodes monophily (Section 2.5).

To understand how MLaP encodes monophily, we consider the example in Fig. 2. In this example, we have three green nodes connected to a yellow node and two nodes of different colors connected to the yellow node. Then, one way to encode monophily in Fig. 2(a) while predicting label for $j_\ell, \ell \in [5]$, is to get a *distribution* of labels of nodes connected to node i thus encoding its neighbors’ distribution. The fact that there are more nodes with green color than other colors can be used by the model to make a prediction. But this information may only sometimes be present, or there may be few labeled nodes around node i . Consequently, we propose to use a model that predicts the label distribution of nodes connected to i . We use the node features (\mathbf{x}_i) and PE (\mathbf{p}_i) of node i to build this model since nodes that are connected to node i share similar labels, and thus, the features of node i must be predictive of its neighbors. So, in Fig. 2(a), we train a model to predict a distribution of i ’s neighbors. Next, we provide j_ℓ the learned distribution of i ’s neighbors by propagating the learned distribution from i back to j_ℓ . Eqs. (1) to (3) correspond to MLaP. We train a final model that leverages this information together with node features and PEs (Fig. 2(b)).

3.2 OUR METHOD: GLINKX

We put the components discussed in Section 3.1 together into three stages. In the first stage, we pre-train the PEs by using KGEs. Next, encode monophily into our model by training a model that predicts a node’s neighbors’ distribution and by propagating the soft labels from the fitted model. Finally, we combine the propagated information, node features, and PEs to train a final model. GLINKX is described in Alg. 1 and consists of three main components detailed as block diagrams in Fig. 1. Fig. 2 shows the GLINKX stages from Alg. 1 on a toy graph:

1st Stage (KGEs): We train DistMult KGEs with Pytorch-Biggraph (Yang et al., 2014) treating G as a knowledge graph with only one relation (see App. A.4 for more details). Here we have decided to use DistMult, but one can use their method of choice to embed the graph.

⁴Positional information can also be provided by other methods such as node2vec (Grover & Leskovec, 2016), however, most of such methods are less scalable.

2nd Stage (MLaP): First (2nd Stage in Alg. 1, Fig. 1(b), and Fig. 2(a)), for a node we want to learn the distribution of *its neighbors*. To achieve this, we propagate the labels from a node’s neighbors (we call this step MLaP Forward), i.e. calculate

$$\hat{\mathbf{y}}_i = \frac{\sum_{j \in V_{\text{train}}: (j,i) \in E_{\text{train}}} \mathbf{y}_j}{|\{j \in V_{\text{train}} : (j,i) \in E_{\text{train}}\}|} \quad \forall i \in V_{\text{train}}. \quad (1)$$

Then, we train a model that predicts the distribution of neighbors, which we denote with $\tilde{\mathbf{y}}_i$ using the ego features $\{\mathbf{x}_i\}_{i \in V_{\text{train}}}$ and the PEs $\{\mathbf{p}_i\}_{i \in V_{\text{train}}}$ and maximize the negative cross-entropy with treating $\{\hat{\mathbf{y}}_i\}_{i \in V_{\text{train}}}$ as ground truth labels, namely we maximize

$$\mathcal{L}_{\text{CE}, 1}(\boldsymbol{\theta}_1) = \sum_{i \in V_{\text{train}}} \sum_{l \in [c]} \hat{\mathbf{y}}_{i,l} \log(\tilde{\mathbf{y}}_{i,l}), \quad (2)$$

where $\tilde{\mathbf{y}}_i = f_1(\mathbf{x}_i, \mathbf{p}_i; \boldsymbol{\theta}_1)$ and $\boldsymbol{\theta}_1 \in \Theta_1$ is a learnable parameter vector. Although in this paper we assume to be in the *transductive setting*, this step allows us to be inductive (see App. B). In Section 3.4 we give a theoretical justification of this step, namely “*why is it good to use a parametric model to predict the distribution of neighbors?*”.

Finally, we propagate the predicted soft-labels $\tilde{\mathbf{y}}_i$ back to the original nodes, i.e. calculate

$$\mathbf{y}'_i = \frac{\sum_{j \in V: (i,j) \in E} \tilde{\mathbf{y}}_j}{|\{j \in V : (i,j) \in E\}|} \quad \forall i \in V_{\text{train}}, \quad (3)$$

where the soft labels $\{\tilde{\mathbf{y}}_i\}_{i \in V_{\text{train}}}$ have been computed with the parameter $\boldsymbol{\theta}_1^*$ of the epoch with the best validation accuracy from model $f_1(\cdot; \boldsymbol{\theta}_1)$. We call this step MLaP Backward.

3rd Stage (Final Model): We make the final predictions $\mathbf{y}_{\text{final}, i} = f_2(\mathbf{x}_i, \mathbf{p}_i, \mathbf{y}'_i; \boldsymbol{\theta}_2)$ by combining the ego embeddings, PEs, and the (back)-propagated soft labels ($\boldsymbol{\theta}_2$ is a learnable parameter vector). We use the soft-labels $\tilde{\mathbf{y}}_i$ instead of the actual labels one-hot (y_i) in order to avoid label leakage, which hurts performance (see also (Shi et al., 2020) for a different way to combat label leakage). Finally, we maximize the negative cross-entropy with respect to a node’s own labels,

$$\mathcal{L}_{\text{CE}, 2}(\boldsymbol{\theta}_2) = \sum_{i \in V_{\text{train}}} \sum_{l \in [c]} \mathbb{I}\{y_i = l\} \log(\mathbf{y}_{\text{final}, i, l}), \quad (4)$$

Overall, Stage 2 corresponds to learning the neighbor distributions and propagating these distributions, and Stage 3 uses these distributions to train a new model which predicts a node’s labels. In Section 3.4, we prove that such a two-step procedure incurs lower errors than directly using the features to predict a node’s labels.

Scalability: GLINKX is highly scalable as it performs message passing a constant number of times by paying an $O(mc)$ cost, where the dimensionality of classes c is usually small (compared to d_X that GCNs rely on). In both Stages 2 and 3 of Alg. 1, we train node-level MLPs, which allow us to leverage i.i.d. (row-wise) mini-batching, like tabular data, and thus our complexity is similar to other shallow methods (LINKX, FSGNN) (Lim et al., 2021; Maurya et al., 2021). This, combined with the propagation outside the training loops, circumvents the scalability issues of GCNs. For more details, refer App. A.3.

3.3 VARYING HOMOPHILY

Graphs with monophily experience homophily, heterophily, or both. For instance, in the yelp-chi dataset – where we classify a review as spam/non-spam (see Fig. 3) – we observe a case of monophily together with varying homophily. Specifically in this dataset, spam reviews are linked to non-spam reviews, and non-spam reviews usually connect to other non-spam reviews, which makes the node homophily distribution bimodal. Here the 2nd-order similarity makes the MLaP mechanism effective.

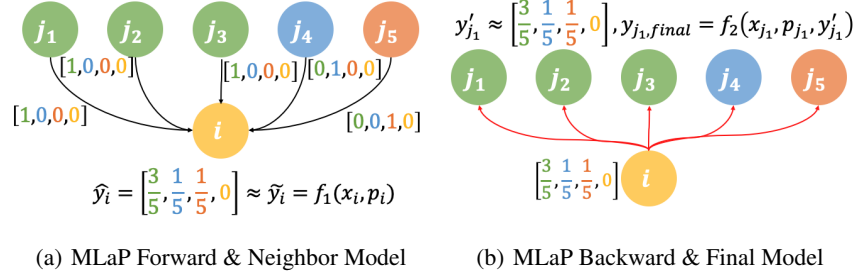
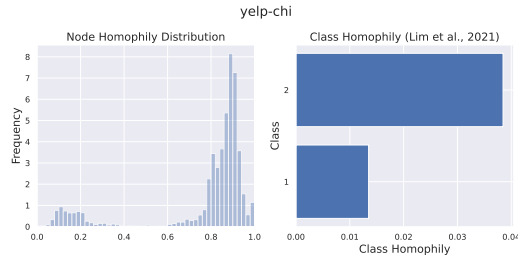
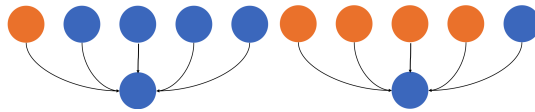


Figure 2: Example. For node i we want to learn a model that takes i 's features $\mathbf{x}_i \in \mathbb{R}^{d_x}$, and PEs $\mathbf{p}_i \in \mathbb{R}^{d_p}$ and predict a value $\tilde{\mathbf{y}}_i \in \mathbb{R}^c$ that matches the label distribution of its neighbors neighbors $\hat{\mathbf{y}}_i$ using a shallow model. Next, we want to propagate (outside the training loop) the (predicted) distribution of a node back to its neighbors and use it together with the ego features and the PEs to make a prediction about a node's own label. We propagate $\tilde{\mathbf{y}}_i$ to its neighbors j_1 to j_5 . For example, for j_1 , we encode the propagated distribution estimate $\tilde{\mathbf{y}}_i$ from i to form \mathbf{y}'_{j_1} . We predict the label by using $\mathbf{y}'_{j_1}, \mathbf{x}_{j_1}, \mathbf{p}_{j_1}$.



(a) Node and class homophily



(b) Homophilous example (c) Heterophilous example

Figure 3: Top: Node and class homophily distributions for the yelp-chi dataset. Bottom: Examples of a homophilous (Fig. 3(b)) and a heterophilous (Fig. 3(c)) region in the same graph that are both monophilous, namely they are connected to many neighbors of the same kind. In a spam network, the homophilous region corresponds to many non-spam reviews connecting to non-spam reviews (which is the expected behaviour of a non-spammer user), and the heterophilous region corresponds to spam reviews targeting non-spam reviews (which is the expected behaviour of spammers), thus, yielding a graph with both homophilous and heterophilous regions such as in Fig. 3(a).

3.4 THEORETICAL ANALYSIS

Justification of Stage 2: In Stage 2, we train a parametric model to learn the distribution of a node’s neighbors from the node features ξ_i ⁵. Arguably, we can learn such a distribution naïvely by counting the neighbors i that belong to each class. This motivates our first theoretical result. In summary, we show that training a parametric model for learning the distribution of a node’s neighbors (as in Stage 2) yields a lower error than the naïve solution. Below we present the Thm. 1 (proof in App. F) for undirected graphs (the case of directed graphs is the same, but we omit it for simplicity of exposition):

Theorem 1. *Let $G([n], E)$ be an undirected graph of minimum degree $K > c^2$ and let $\mathbf{Q}_i \in \Gamma_c$ be the likelihood, from the viewpoint of node i , of any node in its neighborhood $\mathcal{N}(i)$ to be assigned to different classes for every node $i \in [n]$. The following two facts are true (under standard assumptions for SGD and the losses):*

1. *Let $\widehat{\mathbf{Q}}_i$ be the sample average of \mathbf{Q}_i , i.e. $\widehat{\mathbf{Q}}_{i,j} = \frac{1}{|\mathcal{N}(i)|} \sum_{k \in \mathcal{N}(i)} \mathbb{I}\{y_k = j\}$. Then, for every $i \in [n]$, we have that $\max_{j \in [c]} \mathbb{E}[|Q_{i,j} - \widehat{Q}_{i,j}|] \leq \mathbb{E}[\|\mathbf{Q}_i - \widehat{\mathbf{Q}}_i\|_\infty] \leq O\left(\sqrt{\frac{\log(Kc)}{K}}\right)$.*
2. *Let $q(\cdot|\xi_i; \theta)$ be a model parametrized by $\theta \in \mathbb{R}^D$ that uses the features ξ_i of each node i to predict \mathbf{Q}_i . We estimate the parameter θ_1 by running SGD for $t = n$ steps to maximize $\mathcal{L}(\theta) = \frac{1}{n} \sum_{i=1}^n \sum_{j=1}^c Q_{i,j} \log q(j|\xi_i; \theta)$. Then, for every $i \in [n]$, we have that $\max_{j \in [c]} \mathbb{E}[|q(j; \xi_i; \theta_1) - Q_{i,j}|] \leq O\left(\sqrt{\frac{\log n}{n}}\right)$.*

It is evident here that if the minimum degree K is much smaller than n , then the parametric model has lower error than the naïve approach, namely $\tilde{O}(n^{-1/2})$ compared to $\tilde{O}(K^{-1/2})$.

Justification of Stages 2 and 3: We now provide theoretical foundations for the two-stage approach. Specifically, we argue that a two-stage procedure involving learning the distribution of a node’s 2nd-hop neighbor distributions (we assume for simplicity, again, that the graph is undirected) first with a parametric model such as in Thm. 1, and then running a two-phase algorithm to learn a parametric model that predicts a node’s label, yields a lower error than naïvely training a shallow parametric model to learn a node’s labels. The first phase of the two-phase algorithm involves training the model first by minimizing the cross-entropy between the predictions and the 2nd-hop neighborhood distribution. Then the model trains a joint objective that uses the learned neighbor distributions and the actual labels starting from the model learned in the previous phase.

Theorem 2. *Let $G([n], E)$ be an undirected graph of minimum degree $K > c^2$ and, let P_i be the likelihood of node i to be assigned to a different class, and let $\mathbf{Q}_i, q(\cdot|\xi_i; \theta_1)$ defined as in Thm. 1. Let $p(\cdot|\xi_i; \mathbf{w})$ be a model parametrized by $\mathbf{w} \in \mathbb{R}^D$ that is used to predict the class assignments $y_i \sim p(\cdot|\xi_i; \mathbf{w})$. Let \mathbf{w}_* be the optimal parameter. The following are true (under standard assumptions for SGD and the losses):*

1. *The naïve optimization scheme that runs SGD to maximize $\mathcal{G}(\mathbf{w}) = \frac{1}{n} \sum_{i=1}^n \sum_{j=1}^c P_{i,j} \log p(j|\xi_i; \mathbf{w})$ for n steps has error $\mathbb{E}[\mathcal{G}(\mathbf{w}_{n+1}) - \mathcal{G}(\mathbf{w}_*)] \leq O\left(\frac{\log n}{n}\right)$.*
2. *The two-phase optimization scheme that runs SGD to maximize $\widehat{\mathcal{G}}(\mathbf{w}) = \frac{1}{n} \sum_{i=1}^n \sum_{j=1}^c \left(\frac{1}{|\mathcal{N}(i)|} \sum_{k \in \mathcal{N}(i)} q(j|\xi_k; \theta_1)\right) \log p(j|\xi_i; \mathbf{w})$ for n_1 steps, to estimate a solution \mathbf{w}' and then runs SGD on the objective $\lambda \widehat{\mathcal{G}}(\mathbf{w}) + (1 - \lambda) \mathcal{G}(\mathbf{w})$ for n steps starting from \mathbf{w}' , achieves error $\mathbb{E}[\mathcal{G}(\mathbf{w}_{n+1}) - \mathcal{G}(\mathbf{w}_*)] \leq O\left(\frac{\sqrt{\log n \log \log n}}{n}\right)$.*

You can find the proof in App. F. We observe that the two-phase optimization scheme can reduce the error by a factor of $\sqrt{\log n / \log \log n}$ highlighting the importance of using the distribution of the 2nd-hop neighbors of a node to predict its label and holds regardless of the homophily properties of the graph. Also, note that the above two-phase optimization scheme differs from the description of the method we gave in Alg. 1. The difference is that the distribution of a node’s neighbors is embedded into the model in the case of Alg. 1, and the distribution of a node’s neighbors are embedded into the loss function in Thm. 2 as a regularizer. In Alg. 1, we chose to incorporate this information in the model because using multiple losses harms scalability and makes training harder in practice. In the

⁵In Section 3.1, ξ_i s correspond to the augmented features $\xi_i = [\mathbf{x}_i; \mathbf{p}_i]$

same spirit, the conception of GCNs (Kipf & Welling, 2016) replaces explicit regularization with the graph Laplacian with the topology into the model (see also (Hamilton et al., 2017; Yang et al., 2016)).

3.5 COMPLEMENTARITY

Different components of GLINKX provide a *complementary* signal to components proposed in the GNN literature (Maurya et al., 2021; Zhang et al., 2022b; Rossi et al., 2020). One can combine GLINKX with existing architectures (e.g. feature propagations (Maurya et al., 2021; Rossi et al., 2020), label propagations (Zhang et al., 2022b)) for potential metric gains. For example, SIGN computes a series of $r \in \mathbb{N}$ feature propagations $[X, \Phi X, \Phi^2 X, \dots, \Phi^r X]$ where Φ is a matrix (e.g., normalized adjacency or normalized Laplacian) as a preprocessing step. We can include this complementary signal, namely, embed each of the propagated features and combine them in the 3rd Stage to GLINKX. Overall, although in this paper we want to keep GLINKX simple to highlight its main components, we conjecture that adding more components to GLINKX would improve its performance on datasets with highly variable homophily (see Section 3.3).

4 EXPERIMENTS & CONCLUSIONS

Comparisons: We experiment with homophilous and heterophilous datasets (see Tab. 1 and App. D.3). We train KGEs with Pytorch-Biggraph (Lerer et al., 2019; Yang et al., 2014). For homophilous datasets, we compare with vanilla GCN and GAT, FSGNN, and Label Propagation (LP). For a fair comparison, we compare with one-layer GCN/GAT/FSGNN/LP since our method is one-hop. We also compare with higher-order (h.o.) GCN/GAT/FSGNN/LP with 2 and 3 layers. In the heterophilous case, we compare with LINKX⁶ because it is scalable and is shown to work better than other baselines (e.g., H2GCN, MixHop, etc.) and with FSGNN. Note that we do not compare GLINKX with other more complex methods because GLINKX is complementary to them (see Section 3.5), and we can incorporate these designs into GLINKX. We use a *ResNet* module to combine our algorithm’s components from Stages 2 and 3. Details about the hyperparameters we use are in App. C.

In the heterophilous datasets, GLINKX outperforms LINKX (except for arxiv-year, where we are within the confidence interval). Moreover, the performance gap between using KGEs and adjacency embeddings shrinks as the dataset grows. In the homophilous datasets, GLINKX outperforms 1-layer GCN/GAT/LP/FSGNN and LINKX. In PubMed, GLINKX beats h.o. GCN/GAT and in arxiv-year GLINKX is very close to the performance of GCN/GAT.

Finally, we note that our method produces consistent results across regime shifts. In detail, in the heterophilous regime, our method performs on par with LINKX; however, when we shift to the homophilous regime, LINKX’s performance drops, whereas our method’s performance continues to be high. Similarly, while FSGNN performs similarly to GLINKX on the homophilous datasets, we observe a significant performance drop on the heterophilous datasets (see arxiv-year).

Ablation Study: We ablate each component of Alg. 1 to see each component’s performance contribution. We use the hyperparameters of the best model from Tab. 1. We perform two types of ablations: (i) we remove each of the components from all stages of the training, and (ii) we remove the corresponding components only from the 3rd Stage. Except for removing the PEs from the 3rd Stage only on ogbn-arxiv, all components contribute to increased performance on both datasets. Note that adding PEs in the 1st Stage does improve performance, suggesting the primary use case of PEs.

Conclusion: We present GLINKX, a scalable method for node classification in homophilous and heterophilous graphs that combines three components: (i) ego embeddings, (ii) PEs, and (iii) monophilous propagations. As future work, (i) GLINKX can be extended in heterogeneous graphs, (ii) use more expressive methods such as attention or Wasserstein barycenters (Cuturi & Doucet, 2014) for averaging the low-dimensional messages, and (iii) add complementary signals.

⁶We have run our method with hyperparameter space that is a subset of the sweeps reported in (Lim et al., 2021) due to resource constraints. A bigger hyperparameter search would improve our results.

Table 1: Experimental results. (*) = results from the OGB leaderboard.

	Homophilous Datasets		Heterophilous Datasets		
	PubMed	ogbn-arxiv	squirrel	yelp-chi	arxiv-year
n	19.7K	169.3K	5.2K	169.3K	45.9K
m	44.3K	1.16M	216.9K	7.73M	1.16M
Edge-insensitive homophily (Lim et al., 2021)	0.66	0.41	0.02	0.05	0.27
d_X/c	500 / 27	128 / 40	2089 / 5	32 / 2	128 / 5
GLINKX w/ KGEs	87.95 \pm 0.30	69.27 \pm 0.25	45.83 \pm 2.89	87.82 \pm 0.20	54.09 \pm 0.61
GLINKX w/ Adjacency	88.03 \pm 0.30	69.09 \pm 0.13	69.15 \pm 1.87	89.32 \pm 0.45	53.07 \pm 0.29
Label Propagation (1-hop)	83.02 \pm 0.35	69.59 \pm 0.00	32.22 \pm 1.45	85.98 \pm 0.28	43.71 \pm 0.22
LINKX (from (Lim et al., 2021))	87.86 \pm 0.77	67.32 \pm 0.24	61.81 \pm 1.80	85.86 \pm 0.40	56.00 \pm 1.34
LINKX (our runs)	87.55 \pm 0.37	63.91 \pm 0.18	61.46 \pm 1.60	88.25 \pm 0.24	53.78 \pm 0.06
GCN w/ 1 Layer	86.43 \pm 0.74	50.76 \pm 0.20		N/A	
GAT w/ 1 Layer	86.41 \pm 0.53	54.42 \pm 0.10		N/A	
FSGNN w/ 1 Layer	88.93 \pm 0.31	61.82 \pm 0.84	64.06 \pm 2.69	86.36 \pm 0.36	42.86 \pm 0.22
Higher-order GCN	86.29 \pm 0.46	71.18 \pm 0.27 (*)		N/A	
Higher-order GAT	86.64 \pm 0.40	73.66 \pm 0.11 (*)		N/A	
Higher-order FSGNN	89.37 \pm 0.49	69.26 \pm 0.36	68.04 \pm 2.19	86.33 \pm 0.30	44.89 \pm 0.29
Label Propagation (2-hop)	83.44 \pm 0.35	69.78 \pm 0.00	43.41 \pm 1.44	85.95 \pm 0.26	46.30 \pm 0.27
Label Prop. on $\mathbb{I}[A^2 - A - I \geq 0]$	82.14 \pm 0.33	9.87 \pm 0.00	24.43 \pm 1.18	85.68 \pm 0.32	23.08 \pm 0.13

Table 2: Ablation Study. We use the hyperparameters of the best run from Tab. 1 with KGEs.

	Ablation Type	Stages	All	Remove ego embeddings	Remove propagation	Remove PEs
Heterophilous	arxiv-year	All Stages	54.09 \pm 0.61	53.52 \pm 0.77	50.83 \pm 0.24	39.06 \pm 0.35
	arxiv-year	3rd Stage	54.09 \pm 0.61	53.69 \pm 0.65	50.83 \pm 0.24	49.13 \pm 1.10
Homophilous	ogbn-arxiv	All Stages	69.27 \pm 0.25	61.26 \pm 0.33	62.70 \pm 0.34	65.64 \pm 0.18
	ogbn-arxiv	3rd Stage	69.27 \pm 0.25	67.60 \pm 0.39	62.70 \pm 0.34	69.62 \pm 0.15

ACKNOWLEDGEMENTS

The authors would like to thank Maria Gorinova, Fabrizio Frasca, Sophie Hilgard, Ben Chamberlain, and Katarzyna Janocha from Twitter Cortex Applied Research for the useful discussions and comments on our work. MP thanks Jon Kleinberg for providing travel support through the Simons Investigator Grant. MP would also like to thank Felix Hohne for his help regarding questions about the LINKX codebase.

REFERENCES

- Marjan Albooyeh, Rishab Goel, and Seyed Mehran Kazemi. Out-of-sample representation learning for knowledge graphs. In *Findings of the Association for Computational Linguistics: EMNLP 2020*, pp. 2657–2666, 2020.
- Uri Alon and Eran Yahav. On the bottleneck of graph neural networks and its practical implications. In *International Conference on Learning Representations*, 2021. URL <https://openreview.net/forum?id=i800PhOCVH2>.
- Kristen M Altenburger and Johan Ugander. Monophily in social networks introduces similarity among friends-of-friends. *Nature human behaviour*, 2(4):284–290, 2018a.
- Kristen M Altenburger and Johan Ugander. Node attribute prediction: An evaluation of within-versus across-network tasks. In *NeurIPS Workshop on Relational Representation Learning*, 2018b.
- Peter W Battaglia, Jessica B Hamrick, Victor Bapst, Alvaro Sanchez-Gonzalez, Vinicius Zambaldi, Mateusz Malinowski, Andrea Tacchetti, David Raposo, Adam Santoro, Ryan Faulkner, et al. Relational inductive biases, deep learning, and graph networks. *arXiv preprint arXiv:1806.01261*, 2018.
- K. Bhatia, K. Dahiya, H. Jain, P. Kar, A. Mittal, Y. Prabhu, and M. Varma. The extreme classification repository: Multi-label datasets and code, 2016. URL <http://manikvarma.org/downloads/XC/XMLRepository.html>.
- Antoine Bordes, Nicolas Usunier, Alberto Garcia-Duran, Jason Weston, and Oksana Yakhnenko. Translating embeddings for modeling multi-relational data. *Advances in neural information processing systems*, 26, 2013.
- Xavier Bresson and Thomas Laurent. Residual gated graph convnets. *arXiv preprint arXiv:1711.07553*, 2017.
- Eli Chien, Jianhao Peng, Pan Li, and Olgica Milenkovic. Adaptive universal generalized pagerank graph neural network. *arXiv preprint arXiv:2006.07988*, 2020.
- Marco Cuturi and Arnaud Doucet. Fast computation of wasserstein barycenters. In Eric P. Xing and Tony Jebara (eds.), *Proceedings of the 31st International Conference on Machine Learning*, volume 32 of *Proceedings of Machine Learning Research*, pp. 685–693, Beijing, China, 22–24 Jun 2014. PMLR. URL <https://proceedings.mlr.press/v32/cuturi14.html>.
- Francesco Di Giovanni, James Rowbottom, Benjamin P Chamberlain, Thomas Markovich, and Michael M Bronstein. Graph neural networks as gradient flows. *arXiv preprint arXiv:2206.10991*, 2022.
- Yingtong Dou, Zhiwei Liu, Li Sun, Yutong Deng, Hao Peng, and Philip S Yu. Enhancing graph neural network-based fraud detectors against camouflaged fraudsters. In *Proceedings of the 29th ACM International Conference on Information & Knowledge Management*, pp. 315–324, 2020.
- Vijay Prakash Dwivedi, Anh Tuan Luu, Thomas Laurent, Yoshua Bengio, and Xavier Bresson. Graph neural networks with learnable structural and positional representations. *arXiv preprint arXiv:2110.07875*, 2021.
- Ahmed El-Kishky, Thomas Markovich, Serim Park, Chetan Verma, Baekjin Kim, Ramy Eskander, Yury Malkov, Frank Portman, Sofía Samaniego, Ying Xiao, et al. Twhin: Embedding the twitter heterogeneous information network for personalized recommendation. *arXiv preprint arXiv:2202.05387*, 2022.
- Aditya Grover and Jure Leskovec. node2vec: Scalable feature learning for networks. In *Proceedings of the 22nd ACM SIGKDD international conference on Knowledge discovery and data mining*, pp. 855–864, 2016.
- Will Hamilton, Zhitao Ying, and Jure Leskovec. Inductive representation learning on large graphs. *Advances in neural information processing systems*, 30, 2017.

- Weihua Hu, Matthias Fey, Marinka Zitnik, Yuxiao Dong, Hongyu Ren, Bowen Liu, Michele Catasta, and Jure Leskovec. Open graph benchmark: Datasets for machine learning on graphs. *Advances in neural information processing systems*, 33:22118–22133, 2020.
- Qian Huang, Horace He, Abhay Singh, Ser-Nam Lim, and Austin R Benson. Combining label propagation and simple models out-performs graph neural networks. *arXiv preprint arXiv:2010.13993*, 2020.
- Di Jin, Rui Wang, Meng Ge, Dongxiao He, Xiang Li, Wei Lin, and Weixiong Zhang. Raw-gnn: Random walk aggregation based graph neural network. *arXiv preprint arXiv:2206.13953*, 2022a.
- Wei Jin, Lingxiao Zhao, Shichang Zhang, Yozen Liu, Jiliang Tang, and Neil Shah. Graph condensation for graph neural networks. In *International Conference on Learning Representations*, 2022b. URL <https://openreview.net/forum?id=WLEx3Jo4QaB>.
- Jinwoo Kim, Tien Dat Nguyen, Seonwoo Min, Sungjun Cho, Moontae Lee, Honglak Lee, and Seunghoon Hong. Pure transformers are powerful graph learners. *arXiv preprint arXiv:2207.02505*, 2022.
- Thomas N Kipf and Max Welling. Semi-supervised classification with graph convolutional networks. *arXiv preprint arXiv:1609.02907*, 2016.
- Jon M Kleinberg. Authoritative sources in a hyperlinked environment. *Journal of the ACM (JACM)*, 46(5):604–632, 1999.
- Runlin Lei, Zhen Wang, Yaliang Li, Bolin Ding, and Zhewei Wei. Evennet: Ignoring odd-hop neighbors improves robustness of graph neural networks. *arXiv preprint arXiv:2205.13892*, 2022.
- Adam Lerer, Ledell Wu, Jiajun Shen, Timothee Lacroix, Luca Wehrstedt, Abhijit Bose, and Alex Peysakhovich. Pytorch-biggraph: A large scale graph embedding system. *Proceedings of Machine Learning and Systems*, 1:120–131, 2019.
- Guohao Li, Matthias Muller, Ali Thabet, and Bernard Ghanem. Deepgcns: Can gcns go as deep as cnns? In *Proceedings of the IEEE/CVF international conference on computer vision*, pp. 9267–9276, 2019.
- Derek Lim, Felix Hohne, Xiuyu Li, Sijia Linda Huang, Vaishnavi Gupta, Omkar Bhalerao, and Ser Nam Lim. Large scale learning on non-homophilous graphs: New benchmarks and strong simple methods. *Advances in Neural Information Processing Systems*, 34:20887–20902, 2021.
- Sitao Luan, Chenqing Hua, Qincheng Lu, Jiaqi Zhu, Mingde Zhao, Shuyuan Zhang, Xiao-Wen Chang, and Doina Precup. Is heterophily a real nightmare for graph neural networks to do node classification? *arXiv preprint arXiv:2109.05641*, 2021.
- Sunil Kumar Maurya, Xin Liu, and Tsuyoshi Murata. Improving graph neural networks with simple architecture design. *arXiv preprint arXiv:2105.07634*, 2021.
- Miller McPherson, Lynn Smith-Lovin, and James M Cook. Birds of a feather: Homophily in social networks. *Annual review of sociology*, pp. 415–444, 2001.
- Christopher Morris, Martin Ritzert, Matthias Fey, William L Hamilton, Jan Eric Lenssen, Gaurav Rattan, and Martin Grohe. Weisfeiler and leman go neural: Higher-order graph neural networks. In *Proceedings of the AAAI conference on artificial intelligence*, volume 33, pp. 4602–4609, 2019.
- Hongbin Pei, Bingzhe Wei, Kevin Chen-Chuan Chang, Yu Lei, and Bo Yang. Geom-gcn: Geometric graph convolutional networks. *arXiv preprint arXiv:2002.05287*, 2020.
- Everett M Rogers, Arvind Singhal, and Margaret M Quinlan. Diffusion of innovations. In *An integrated approach to communication theory and research*, pp. 432–448. Routledge, 2014.
- Emanuele Rossi, Fabrizio Frasca, Ben Chamberlain, Davide Eynard, Michael Bronstein, and Federico Monti. Sign: Scalable inception graph neural networks. *arXiv preprint arXiv:2004.11198*, 7:15, 2020.

- Benedek Rozemberczki, Carl Allen, and Rik Sarkar. Multi-scale attributed node embedding. *Journal of Complex Networks*, 9(2):cnab014, 2021.
- Prithviraj Sen, Galileo Namata, Mustafa Bilgic, Lise Getoor, Brian Galligher, and Tina Eliassi-Rad. Collective classification in network data. *AI magazine*, 29(3):93–93, 2008.
- Yunsheng Shi, Zhengjie Huang, Shikun Feng, Hui Zhong, Wenjin Wang, and Yu Sun. Masked label prediction: Unified message passing model for semi-supervised classification. *arXiv preprint arXiv:2009.03509*, 2020.
- Arnab Sinha, Zhihong Shen, Yang Song, Hao Ma, Darrin Eide, Bo-June Hsu, and Kuansan Wang. An overview of microsoft academic service (mas) and applications. In *Proceedings of the 24th international conference on world wide web*, pp. 243–246, 2015.
- Balasubramaniam Srinivasan and Bruno Ribeiro. On the equivalence between positional node embeddings and structural graph representations. *arXiv preprint arXiv:1910.00452*, 2019.
- Chuxiong Sun, Hongming Gu, and Jie Hu. Scalable and adaptive graph neural networks with self-label-enhanced training. *arXiv preprint arXiv:2104.09376*, 2021.
- Petar Veličković, Guillem Cucurull, Arantxa Casanova, Adriana Romero, Pietro Lio, and Yoshua Bengio. Graph attention networks. *arXiv preprint arXiv:1710.10903*, 2017.
- Keyulu Xu, Weihua Hu, Jure Leskovec, and Stefanie Jegelka. How powerful are graph neural networks? In *International Conference on Learning Representations*, 2019. URL <https://openreview.net/forum?id=ryGs6iA5Km>.
- Bishan Yang, Wen-tau Yih, Xiaodong He, Jianfeng Gao, and Li Deng. Embedding entities and relations for learning and inference in knowledge bases. *arXiv preprint arXiv:1412.6575*, 2014.
- Zhilin Yang, William Cohen, and Ruslan Salakhudinov. Revisiting semi-supervised learning with graph embeddings. In *International conference on machine learning*, pp. 40–48. PMLR, 2016.
- Shichang Zhang, Yozen Liu, Yizhou Sun, and Neil Shah. Graph-less neural networks: Teaching old MLPs new tricks via distillation. In *International Conference on Learning Representations*, 2022a. URL https://openreview.net/forum?id=4p6_5HBWPCw.
- Wentao Zhang, Ziqi Yin, Zeang Sheng, Yang Li, Wen Ouyang, Xiaosen Li, Yangyu Tao, Zhi Yang, and Bin Cui. Graph attention multi-layer perceptron. *Proceedings of the 28th ACM SIGKDD Conference on Knowledge Discovery and Data Mining*, 2022b.
- Wenqing Zheng, Edward W Huang, Nikhil Rao, Sumeet Katariya, Zhangyang Wang, and Karthik Subbian. Cold brew: Distilling graph node representations with incomplete or missing neighborhoods. In *International Conference on Learning Representations*, 2022a. URL <https://openreview.net/forum?id=1ugNpm7W6E>.
- Xin Zheng, Yixin Liu, Shirui Pan, Miao Zhang, Di Jin, and Philip S Yu. Graph neural networks for graphs with heterophily: A survey. *arXiv preprint arXiv:2202.07082*, 2022b.
- Zhiqiang Zhong, Sergey Ivanov, and Jun Pang. Simplifying node classification on heterophilous graphs with compatible label propagation. *arXiv preprint arXiv:2205.09389*, 2022.
- Jiong Zhu, Yujun Yan, Lingxiao Zhao, Mark Heimann, Leman Akoglu, and Danai Koutra. Beyond homophily in graph neural networks: Current limitations and effective designs. *Advances in Neural Information Processing Systems*, 33:7793–7804, 2020.
- Jiong Zhu, Ryan A Rossi, Anup Rao, Tung Mai, Nedim Lipka, Nesreen K Ahmed, and Danai Koutra. Graph neural networks with heterophily. In *Proceedings of the AAAI Conference on Artificial Intelligence*, volume 35, pp. 11168–11176, 2021.

Supplementary Material

A MODEL ADDENDUM

A.1 GRAPH MINI-BATCHING & SHALLOW METHODS

To train a GCN-based model (or generally, whenever propagations based on the graph topology are involved in the model) on a large network (that cannot fit in the GPU memory), one has to do *minibatching* through *neighbor sampling*. For large-scale networks, mini-batching takes much longer than full-batch training, which is one of the reasons that graph GCNs are not preferred in real-world settings (see, e.g., (Jin et al., 2022b; Zhang et al., 2022a; Zheng et al., 2022a; Lim et al., 2021; Maurya et al., 2021; Rossi et al., 2020)).

For this reason, most methods that can scale on real-world settings are *shallow*. *Shallow* (or node-level) models are based on manipulating the node features \mathbf{X} and the graph topology \mathbf{A} so that propagations do not occur during training. Examples of these methods are LINKX, FSGNN (Maurya et al., 2021), and SIGN (Rossi et al., 2020). Such methods treat the input embeddings as tabular data and pass them through a feed-forward neural network (MLP) to produce the predictions. Thus, they avoid the need for neighborhood sampling and instead rely on simple tabular mini-batching.

A.2 RELATIONSHIP TO LABEL PROPAGATION

From a label propagation perspective, one could argue that our method is related to the HITS algorithm of Kleinberg (1999). Besides, on a directed graph, a potential solution would be to perform label propagation with the Gram matrix $\mathbf{A}\mathbf{A}^T$ and use this information as the propagated labels instead of \mathbf{y}'_i . This, however, would not be inductive.

A.3 SCALABILITY

Table 3: Inference Complexity (on the whole dataset) for various methods. The adjacency matrix \mathbf{A} is given in sparse (CSR) format.

Method	Inference Complexity
GLINKX	$O(mc + n(d_X h + h^2 L_X + d_P h + h^2 L_P + h^2 L_{agg}))$
LINKX	$O(md + n(d_X h + h^2 L_X + h^2 L_{agg}))$
L -layer GCN	$O(mdL + nd^2 L)$
L -hop SIGN/FSGNN	$O(nL(nd + d^2 h + L_{agg} h^2))$
L -hop τ -iteration Label Propagation	$O((n + m)cL\tau)$

Cost of 1st Stage: For the 1st Stage, we are using Pytorch-Biggraph to train PEs such as TransE (Bordes et al., 2013), DistMult (Yang et al., 2014). Please refer to (Lerer et al., 2019) for more information.

Cost of 2st Stage: For the 2nd Stage we pay **once** $O(m_{\text{train}}c)$ ($m_{\text{train}} = |E_{\text{train}}|$ is the number of edges in the graph induced by the train nodes) to do perform MLaP Forward and then the MLP that takes \mathbf{x}_i and \mathbf{p}_i with L_X layers for the features \mathbf{x}_i and L_P layers for the PEs \mathbf{p}_i , and L_{agg} layers for the ResNet and hidden dimension h , has forward pass complexity $O(n(d_X h + h^2 L_X + d_P h + h^2 L_P + h^2 L_{agg}))$. Finally, MLaP Backward costs $O(m_{\text{train}}c)$, similarly to MLaP Forward.

Cost of 3rd Stage: The final model costs $O(n(d_X h + h^2 L_X + d_P h + h^2 L_P + ch + h^2 L_{prop} + h^2 L_{agg}))$ for a forward pass of the MLP, where c is the class dimensionality and L_{prop} are the layers for the MLP handling the propagated labels \mathbf{y}'_i .

Inference Complexity: Tab. 3 shows the inference complexity of GLINKX and compares it with the complexity of other methods such as LINKX, L -layer GCN, L -hop FSGNN/SIGN and LP.

Compared to LINKX we pay an $O(m_{\text{train}}c)$ extra cost once. Regarding embedding the adjacency matrix LINKX pays a $O(mh + nh^2 L_P)$ cost for generating the h -dimensional adjacency embeddings

whereas we pay $O(nd_P h + nh^2 L_P)$ which is better for $d_P = O(m/n)$. This holds in most real-world large networks since $d_P \sim 10^2$ whereas $n \sim 1\text{B}$ and $m \sim 100\text{B}$. Also note that using KGEs as PEs has an additional benefit, since KGEs can be trained only *once* and can be used off-the-shelf for other downstream tasks. An L -layer GNN propagates using the adjacency matrix \mathbf{A} and multiplies with a projection matrix $\mathbf{W}^{(i)}$ (for each layer) thus achieving an $O(dLm + nd^2L)$ complexity; the former term is due to the propagation (assuming \mathbf{A} is sparse), and the latter term accounts for the multiplication with the projection matrix. The L -hop SIGN (resp. L -hop FSGNN) performs L (resp. $2L$) propagations of the feature matrix \mathbf{X} using a sequence of matrices $\{\Phi^\ell\}_{\ell \in [L]}$ which cost a total of $O(n^2 dL)$ (assuming the matrices are dense), and then uses a ResNet with L_{agg} layers block to concatenate the propagated features, which costs $O(nLdhL_{\text{agg}})$, yielding an inference complexity cost of $O(nL(nd + d^2h + L_{\text{agg}}h^2))$. Finally, Label Propagation with sparse matrices costs $O((n+m)cL\tau)$, where τ is the number of iterations of the LP algorithm.

A.4 KNOWLEDGE GRAPH EMBEDDING TRAINING

In the sequel, we provide a general algorithm for training KGEs to be used as positional embedding \mathbf{P} . Briefly we treat G as a knowledge graph with only one relation $r = \rho$. Specifically, each edge $(u, v) \in E$ corresponds to a head entity with embedding $\mathbf{h} = \mathbf{p}_u$ and a tail entity with embedding $\mathbf{t} = \mathbf{p}_v$. Without loss of generality we can pick $\rho = \mathbf{1}$ to be the vector of all 1s since the constants per dimension can be absorbed by the positional embeddings.

Algorithm 2 Knowledge Graph Embedding Training

Input: Graph $G(V, E)$, Embedding dimension d_P , Comparison function $f : \mathbb{R}^{d_P} \times \mathbb{R}^{d_P} \times \mathbb{R}^{d_P} \rightarrow \mathbb{R}$, Sample loss function $\ell : \mathbb{R} \times \mathbb{R} \rightarrow \mathbb{R}$, Number of epochs T , Batch Size B , Number of negative samples ν
Output: Positional Embeddings $\mathbf{P} \in \mathbb{R}^{n \times d_P}$
 Randomly, initialize the entity embedding matrix $\mathbf{P} \in \mathbb{R}^{n \times d_P}$ with row vectors \mathbf{p}_u for all $u \in V$.
 Let $\rho = \mathbf{1}$
 For each epoch $t \in [T]$, sample minibatches $\{E_{\text{batch}}\}$ of the edges E of size B .

1. For each minibatch E_{batch} and each $(u, v) \in E$ sample ν negative samples $(u'_i, v'_i) \notin E$ and build $T_{\text{batch}} = \bigcup_{i \in [\nu]} \{(u, v), (u'_i, v'_i)\}$
2. Update the embeddings \mathbf{P} wrt

$$\nabla_{\mathbf{P}} \sum_{((u,v), (u',v')) \in T_{\text{batch}}} \ell(f(\mathbf{p}_u, \rho, \mathbf{p}_v), f(\mathbf{p}'_{u'}, \rho, \mathbf{p}'_{v'}))$$

Output \mathbf{P}

In our case, we have chosen the DistMult embeddings Yang et al. (2014) which correspond to choosing the triple product

$$f(\mathbf{h}, \mathbf{r}, \mathbf{t}) = \sum_{i \in d_P} h_i r_i t_i$$

as a comparison function, and the margin-based ranking loss $\ell(f(\mathbf{h}, \mathbf{r}, \mathbf{t}), f(\mathbf{h}', \mathbf{r}, \mathbf{t}')) = \max\{0, \gamma + f(\mathbf{h}, \mathbf{r}, \mathbf{t}) - f(\mathbf{h}', \mathbf{r}, \mathbf{t}')\}$ where γ is the margin.

B INDUCTIVE GLINKX

In the paper we focus on the transductive setting. Here we show how we can extend our framework to the inductive setting. In the inductive setting, during training we only have access to the training graph $G_{\text{train}}(V_{\text{train}}, E_{\text{train}})$. During test, the whole graph $G \subseteq G_{\text{train}}$ is revealed and we make predictions for the test set. The stages of GLINKX in the inductive setting are as follows

1st Stage. For the KGE pretraining Stage, we train KGEs on G_{train} . Then we can use existing methods in the literature such as (El-Kishky et al., 2022; Albooyeh et al., 2020) to infer the KGEs of the test nodes.

2nd Stage. We train the model that predicts the distribution of the neighbors on G_{train} as in Alg. 1. Then for the test nodes, we know their ego features \mathbf{x}_i and we can also infer their PEs (see above) from the pre-trained PEs on the training set. We use these and the pre-trained shallow model in order to predict $\tilde{\mathbf{y}}_i$ for the test nodes. Then, we run MLaP backward to compute \mathbf{y}'_i .

3rd Stage. First, we train the second shallow model by using the propagated soft-predictions only on G_{train} . We then use the ego features, PEs and the propagated information \mathbf{y}'_i to make predictions on the test set.

Alg. 3 shows the process of making predictions on the test set.

Algorithm 3 Inductive GLINKX

Input: Graph $G(V, E)$ with train set $V_{\text{train}} \subseteq V$ and test set $V_{\text{test}} \subseteq V$, node features X , labels Y

Output: Predictions for all nodes $i \in V_{\text{test}}$

Pre-training. Call Alg. 1 with input graph $G_{\text{train}}(V_{\text{train}}, E_{\text{train}})$ and compute PEs $\{\mathbf{p}_i\}_{i \in V_{\text{train}}}$, and pre-trained models f_1 (from 2nd Stage) and f_2 (from 3rd Stage)

1st Stage. Create PEs $\{\mathbf{p}_i\}_{i \in V_{\text{test}}}$ for the nodes of the test set (see e.g. (El-Kishky et al., 2022; Albooyeh et al., 2020))

2nd Stage. Predict the distribution of neighbors for the nodes of the test set as $\tilde{\mathbf{y}}_i = f_1(\mathbf{x}_i, \mathbf{p}_i)$ for all $i \in V_{\text{test}}$. Calculate $\mathbf{y}'_i = \frac{\sum_{j \in V: (i,j) \in E} \tilde{\mathbf{y}}_j}{|\{j \in V: (i,j) \in E\}|}$ for all $i \in V_{\text{test}}$ (MLaP Backward).

3rd Stage. Compute $\mathbf{y}_{\text{final},i} = f_2(\mathbf{x}_i, \mathbf{p}_i, \mathbf{y}'_i)$ for all $i \in V_{\text{test}}$.

Return $\{\mathbf{y}_{\text{final},i}\}_{i \in V_{\text{test}}}$

C HYPERPARAMETERS

For each of the methods we train for 200 epochs and report the test set accuracy on the epoch with the best validation accuracy.

C.1 KGES

We use the following hyperparameters for the KGEs using Pytorch-Biggraph:

- dimension = 400
- 50 epochs
- negative samples = 1000
- batch size = 10000
- dot comparator, softmax loss (Yang et al., 2014)
- learning rate = 0.1

C.2 GLINKX w/ ADJACENCY

C.2.1 SWEEPS

We perform the following sweeps:

- `glinkx_init_layers_X` $\in \{1, 2\}$
- `glinkx_init_layers_A` $\in \{1, 2\}$
- `glinkx_init_layers_agg` $\in \{1, 2\}$
- `glinkx_inner_dropout` $\in \{0.5\}$
- `lr` $\in \{0.1, 0.001\}$

- optimize:r: AdamW

name	init_layers_A	init_layers_X	init_layers_agg	inner_dropout	lr
arxiv-year	1	2	1	0.5	0.001
PubMed	1	2	1	0.5	0.001
squirrel	2	1	1	0.5	0.001
yelp-chi	2	2	1	0.5	0.01

Table 4: GLINKX w/ Adjacency Hyperparameters

C.3 GLINKX w/ KGEs

C.3.1 SWEEPS

We perform the following sweeps for all datasets

- `glinkx_init_layers_X` $\in \{1, 2\}$
- `glinkx_init_layers_A` $\in \{1, 2\}$
- `glinkx_init_layers_agg` $\in \{1, 2\}$
- `glinkx_inner_dropout` : $\in \{0.5\}$
- `lr` $\in \{0.1, 0.001\}$
- optimize:r: AdamW
- `biggraph_vector_length`: 400

name	biggraph_vector_length	init_layers_A	init_layers_X	init_layers_agg	inner_dropout	lr
arxiv-year	400	2	1	1	0.5	0.01
ogbn-arxiv	400	2	2	2	0.5	0.001
PubMed	400	2	2	2	0.5	0.01
squirrel	400	2	1	2	0.5	0.001
yelp-chi	400	2	2	2	0.5	0.01

Table 5: GLINKX w/ Biggraph Hyperparameters

C.4 GAT

C.4.1 SWEEPS

- `gat_num_layers` $\in \{1\}$
- `gat_hidden_channels` $\in \{4, 8, 16, 32\}$
- `gat_num_heads` $\in \{2, 4\}$
- `lr` $\in \{0.01, 0.001\}$

name	gat_heads	gat_hidden_channels	gat_num_layers	lr
arxiv-year	4	8	1	0.1
ogbn-arxiv	4	4	1	0.1
PubMed	4	16	1	0.1
squirrel	4	4	1	0.1

Table 6: GAT w/ 1 layer Hyperparameters

C.5 GCN

C.5.1 SWEEPS

We perform the following sweeps:

- `gcn_num_layers` $\in \{1\}$
- `gcn_hidden_channels` $\in \{4, 8, 16, 32, 64\}$
- `lr` $\in \{0.01, 0.001\}$

name	gcn_hidden_channels	gcn_num_layers	lr
arxiv-year	64	1	0.01
ogbn-arxiv	64	1	0.01
PubMed	64	1	0.01
squirrel	64	1	0.01
yelp-chi	64	1	0.01

Table 7: GCN w/ 1 layer Hyperparameter

C.6 FSGNN

We run the following sweeps for FSGNN

- `layers` = 1 for the 1-layer case and `layers` $\in \{2, 3\}$ for the higher-order case
- `hidden channels` $\in \{32, 64, 128\}$
- `learning rate` $\in \{0.01, 0.001\}$
- `layer normalization` $\in \{\text{true}, \text{false}\}$

C.7 LABEL PROPAGATION

We run the following sweeps using the implementation of Label Propagation from (Lim et al., 2021):

- `α` $\in \{0.01, 0.1, 0.25, 0.5, 0.75, 0.99\}$
- `hops` $\in \{1, 2\}$

D EXPERIMENTS ADDENDUM

D.1 IMPLEMENTATION AND ENVIRONMENT

GLINKX is implemented in Pytorch-Geometric. For the knowledge graph embeddings we use the official Pytorch-Bigraph implementation. We use the official implementation of LINK. For hardware we used Vertex AI notebooks with 8 NVIDIA Tesla V100 with 16GB of memory and 96 CPUs.

D.2 EXPERIMENTAL PROTOCOL

Error Bars. For the PubMed dataset and the heterophilous datasets provided by (Pei et al., 2020; Lim et al., 2021; Yang et al., 2016) we used the fixed splits provided with a fixed seed. For the OGB datasets, where there exists only one officialy released split for each dataset (Hu et al., 2020) we generate the error bars by running the respective experiments with 10 different seeds (0-9).

D.3 DATASETS

For our experiments we use the following datasets (see Tab. 1 for the dataset statistics):

- *PubMed* (Yang et al., 2016; Sen et al., 2008). The PubMed dataset consists of scientific publications from PubMed database pertaining to diabetes classified into one of three classes. Each node is described by a TF-IDF weighted word vector from a dictionary which consists of 500 unique words.
- *ogbn-arxiv* (Hu et al., 2020; Bhatia et al., 2016; Sinha et al., 2015). The ogbn-arxiv dataset is a directed graph, representing the citation network between all CS papers on arxiv mined from the Microsoft Academic Graph (MAG). Nodes are papers and edges correspond to citations. The node features correspond to the average of word embeddings of the title and abstract of the papers. The task is to predict the papers’ subcategories (e.g. CS.LG, CS.SI etc.).
- *squirrel* (Rozemberczki et al., 2021). The data represents page-to-page networks on squirrels mined from Wikipedia between October 2017 and November 2018. Node represent articles and edges are mutual links between the pages. The features of each node are binary and represent the existence of informative nouns that appear on the corresponding Wikipedia pages.
- *arxiv-year, yelp-chi* (Lim et al., 2021). The arXiv-year dataset is derived from the ogbn-arxiv dataset where the labels have been changed in order to convert the dataset from homophilous to heterophilous. Instead of predicting each paper’s subcategories, the new task focuses on predicting the year that a paper is posted, where batches of years have been converted to labels. The yelp-chi dataset includes hotel and restaurant reviews filtered (spam) and recommended (legitimate) by Yelp. The graph structure comes from (Dou et al., 2020) and the features from (Sen et al., 2008). The task is to predict whether a review is a spam or not.

E STAGES DIAGRAM

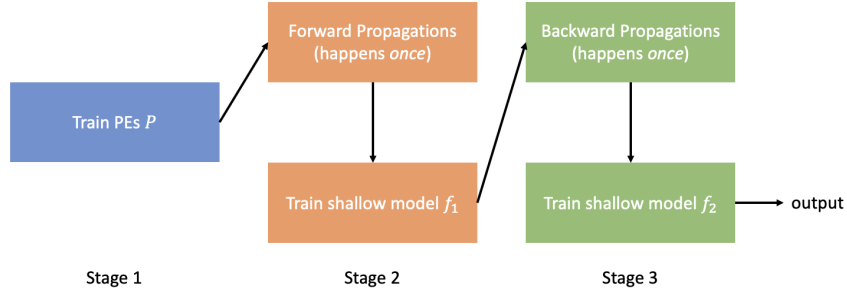


Figure 4: GLINKX stages.

F PROOFS

F.1 PROOF OF THM. 1 (PARAMETRIC ESTIMATION OF Q)

Counting Estimator. As the first step, we can estimate Q_i , denoted by \hat{Q}_i by taking the average class assignment in its neighbor $\mathcal{N}(i)$, i.e.

$$\hat{Q}_{i,j} = \frac{1}{|\mathcal{N}(i)|} \sum_{k \in \mathcal{N}(i)} \mathbb{I}\{y_k = j\}$$

Evidently, $\mathbb{E}[\hat{Q}_{i,j}] = Q_{i,j}$. Also, using Hoeffding concentration inequality, we have, with a probability at least $1 - \delta$,

$$\left| \hat{Q}_{i,j} - \frac{1}{|\mathcal{N}(i)|} \sum_{k \in \mathcal{N}(i)} P_{k,j} \right| \leq \sqrt{\frac{1}{2K} \log \frac{2}{\delta}}$$

Since

$$Q_i = \frac{1}{|\mathcal{N}(i)|} \sum_{k \in \mathcal{N}(i)} P_k$$

we have

$$\|\widehat{\mathbf{Q}}_i - \mathbf{Q}_i\|_\infty \leq \sqrt{\frac{1}{2K} \log \frac{2c}{\delta}}$$

with probability at least $1 - \delta$. Therefore, by the law of total expectation and by minimizing wrt δ , we get

$$\max_{j \in [c]} \mathbb{E}[|Q_{ij} - \widehat{Q}_{ij}|] \leq \mathbb{E}[\|\mathbf{Q}_i - \widehat{\mathbf{Q}}_i\|_\infty] \leq \min_{\delta \in (0,1)} \sqrt{\frac{1}{2K} \log \frac{2c}{\delta}} + \delta \leq O\left(\sqrt{\frac{\log(Kc)}{K}}\right)$$

Parametric Estimator. As the first step, we show that through a parametric optimization, we will be able to obtain a better estimation of \mathbf{Q}_i . In particular, we assume that all \mathbf{Q}_i can be written in the parametric form $q(j|\boldsymbol{\xi}_i; \boldsymbol{\theta})$, where $\boldsymbol{\theta} \in \mathbb{R}^D$ is the parameter of the model. Let $\boldsymbol{\theta}_*$ be the optimal model parameter such that $Q_{i,j} = q(j|\boldsymbol{\xi}_i; \boldsymbol{\theta}_*)$. We define the following loss function

$$\mathcal{L}(\boldsymbol{\theta}) = -\frac{1}{n} \sum_{i=1}^n \sum_{j=1}^c Q_{i,j} \log q(j|\boldsymbol{\xi}_i; \boldsymbol{\theta})$$

Evidently, $\boldsymbol{\theta}_*$ is the minimizer of $\mathcal{L}(\boldsymbol{\theta})$. We assume that $\mathcal{L}(\boldsymbol{\theta})$ is L smooth and γ -PL function, i.e.

$$\|\nabla \mathcal{L}(\boldsymbol{\theta})\| \leq L, \quad \mathcal{L}(\boldsymbol{\theta}) - \mathcal{L}(\boldsymbol{\theta}_*) \leq \frac{1}{2\gamma} \|\nabla \mathcal{L}(\boldsymbol{\theta})\|^2$$

The real objective function $\widehat{\mathcal{L}}(\boldsymbol{\theta})$ based on the observation of class assignments is given as

$$\widehat{\mathcal{L}}(\boldsymbol{\theta}) = -\frac{1}{n} \sum_{i=1}^n \sum_{j=1}^c \widehat{Q}_{i,j} \log q(j|\boldsymbol{\xi}_i; \boldsymbol{\theta})$$

To find the optimal $\boldsymbol{\theta}$, we run stochastic gradient descent. At each iteration t , we sample one node i_t , and compute the gradient \mathbf{g}_t as

$$\mathbf{g}_t = \sum_{j=1}^c \widehat{Q}_{i_t,j} \nabla_{\boldsymbol{\theta}} \log q(j|x_{i_t}; \boldsymbol{\theta})$$

and update the solution by

$$\boldsymbol{\theta}_{t+1} = \boldsymbol{\theta}_t - \eta \mathbf{g}_t$$

where η is a fixed step size whose value will be decided later. We have

$$\begin{aligned} & \mathbb{E}[\mathcal{L}(\boldsymbol{\theta}_{t+1}) - \mathcal{L}(\boldsymbol{\theta}_t)] \\ & \leq \mathbb{E}[\langle \nabla \mathcal{L}(\boldsymbol{\theta}_t), \boldsymbol{\theta}_{t+1} - \boldsymbol{\theta}_t \rangle] + \frac{L}{2} \mathbb{E}[\|\boldsymbol{\theta}_{t+1} - \boldsymbol{\theta}_t\|^2] \\ & = -\eta \left(1 - \frac{\eta L}{2}\right) \mathbb{E}[\|\nabla \mathcal{L}(\boldsymbol{\theta}_t)\|^2] + \frac{\eta^2 L}{2} \mathbb{E}[\|\mathbf{g}_t - \mathbf{g}'_t\|^2 + \|\mathbf{g}'_t - \nabla \mathcal{L}(\boldsymbol{\theta}_t)\|^2] \end{aligned}$$

where $\mathbf{g}'_t = \sum_{j=1}^c Q_{i_t,j} \nabla_{\boldsymbol{\theta}} \log q(j|x_{i_t}; \boldsymbol{\theta})$. We assume that $\|\nabla_{\boldsymbol{\theta}} \log q(j|\boldsymbol{\xi}_i; \boldsymbol{\theta})\| \leq G$ for any $\boldsymbol{\theta}$ and any i . We have

$$\mathbb{E}[\|\mathbf{g}_t - \mathbf{g}'_t\|^2] \leq \left(\frac{c^2}{K} \log \frac{2}{\delta} + \delta\right) G^2, \quad \mathbb{E}[\|\mathbf{g}'_t - \nabla \mathcal{L}(\boldsymbol{\theta}_t)\|^2] \leq G^2$$

By choosing $\delta = c^2/K$, we have

$$\mathbb{E}[\|\mathbf{g}_t - \mathbf{g}'_t\|^2] \leq \frac{2c^2 G^2}{K} \log \frac{2K}{c^2}$$

Putting the above bounds together, we have

$$\mathbb{E}[\mathcal{L}(\boldsymbol{\theta}_{t+1}) - \mathcal{L}(\boldsymbol{\theta}_t)] \leq -\eta \left(1 - \frac{\eta L}{2}\right) \mathbb{E}[\|\nabla \mathcal{L}(\boldsymbol{\theta}_t)\|^2] + \frac{\eta^2 G^2 L}{2} \left(1 + \frac{2c^2}{K} \log \frac{2K}{c^2}\right)$$

Assume $\eta L \leq 1$. Using the fact

$$\mathcal{L}(\boldsymbol{\theta}_t) - \mathcal{L}(\boldsymbol{\theta}_*) \leq \frac{1}{2\gamma} \|\nabla \mathcal{L}(\boldsymbol{\theta}_t)\|^2$$

we have

$$\mathbb{E}[\mathcal{L}(\boldsymbol{\theta}_{t+1}) - \mathcal{L}(\boldsymbol{\theta}_*)] \leq \left(1 - \frac{\eta\gamma}{4}\right) \mathbb{E}[\mathcal{L}(\boldsymbol{\theta}_t) - \mathcal{L}(\boldsymbol{\theta}_*)] + \frac{\eta^2 G^2 L}{2} \left(1 + \frac{2c^2}{K} \log \frac{2K}{c^2}\right)$$

and therefore

$$\mathbb{E}[\mathcal{L}(\boldsymbol{\theta}_{t+1}) - \mathcal{L}(\boldsymbol{\theta}_*)] \leq \exp\left(-\frac{\eta\gamma t}{4}\right) (\mathcal{L}(\boldsymbol{\theta}_0) - \mathcal{L}(\boldsymbol{\theta}_*)) + \frac{\eta G^2 L}{2} \left(1 + \frac{2c^2}{K} \log \frac{2K}{c^2}\right)$$

Let $\boldsymbol{\theta}_1 = \boldsymbol{\theta}_{n+1}$. By choosing

$$\eta = \frac{4}{n\gamma} \log\left(\frac{n\gamma(\mathcal{L}(\boldsymbol{\theta}_0) - \mathcal{L}(\boldsymbol{\theta}_*))}{2G^2 L(1 + 2c^2/K \log(2K/c^2))}\right)$$

we have

$$\mathbb{E}[\mathcal{L}(\boldsymbol{\theta}_1) - \mathcal{L}(\boldsymbol{\theta}_*)] \leq \frac{2G^2 L}{n\gamma} \left(1 + \frac{2c^2}{K} \log \frac{2K}{c^2}\right) \log \frac{n\gamma(\mathcal{L}(\boldsymbol{\theta}_0) - \mathcal{L}(\boldsymbol{\theta}_*))}{2G^2 L(1 + 2c^2/K \log(2K/c^2))} = O\left(\frac{\log n}{n\gamma}\right)$$

Since

$$\mathcal{L}(\boldsymbol{\theta}_1) - \mathcal{L}(\boldsymbol{\theta}_*) = \frac{1}{n} \sum_{i=1}^n \sum_{j=1}^c q(j|\boldsymbol{\xi}_i; \boldsymbol{\theta}_*) \log \frac{q(j|\boldsymbol{\xi}_i; \boldsymbol{\theta}_1)}{q(j|\boldsymbol{\xi}_i; \boldsymbol{\theta}_*)} = \frac{1}{n} \sum_{i=1}^n \sum_{j=1}^c \text{KL}(q(\cdot|\boldsymbol{\xi}_i; \boldsymbol{\theta}_*) \| q(\cdot|\boldsymbol{\xi}_i; \boldsymbol{\theta}_1))$$

and (by Pinsker's Inequality),

$$\text{KL}(q(\cdot|\boldsymbol{\xi}_i; \boldsymbol{\theta}_*) \| q(\cdot|\boldsymbol{\xi}_i; \boldsymbol{\theta}_1)) \geq 2 \left(\sum_{j=1}^c |q(j|\boldsymbol{\xi}_i; \boldsymbol{\theta}_1) - q(j|\boldsymbol{\xi}_i; \boldsymbol{\theta}_*)| \right)^2$$

we have

$$\frac{1}{n} \sum_{i=1}^n \mathbb{E} \left[\left(\sum_{j=1}^c |q(j|\boldsymbol{\xi}_i; \boldsymbol{\theta}_1) - Q_{i,j}| \right)^2 \right] \leq \frac{C \log n}{n\gamma}$$

where

$$C = G^2 L \left(1 + \frac{2c^2}{K} \log \frac{2K}{c^2}\right) \log \frac{\gamma(\mathcal{L}(\boldsymbol{\theta}_0) - \mathcal{L}(\boldsymbol{\theta}_*))}{2G^2 L(1 + 2c^2/K \log(2K/c^2))}$$

Hence, on average, we have

$$|q(j|\boldsymbol{\xi}_i; \boldsymbol{\theta}_1) - Q_{i,j}| \leq \sqrt{\frac{C \log n}{n\gamma}}$$

which could be significantly smaller than $O(1/\sqrt{K})$ when $n \gg K$, indicating that through the parametric modeling of $Q_{i,j}$ and optimization of $\hat{\mathcal{L}}(\boldsymbol{\theta})$, we will be able to achieve significantly better estimation of $Q_{i,j}$ than a simple counting. \square

F.2 PROOF OF THM. 2 (PARAMETRIC ESTIMATION OF P)

Naïve Approach. We now will utilize the estimation $q(\cdot|\boldsymbol{\xi}_i; \boldsymbol{\theta}_1)$ further estimate P_i . Similar to last section, we introduce a parametric estimator $p(j|\boldsymbol{\xi}_i; \boldsymbol{w})$, where $\boldsymbol{w} \in \mathbb{R}^d$ is the parameter. We denote by \boldsymbol{w}_* the optimal parameter, i.e. $P_{i,j} = p(j|\boldsymbol{\xi}_i; \boldsymbol{w}_*)$. Let $\mathcal{G}(\boldsymbol{w})$ be the objective function based on population average, i.e.

$$\mathcal{G}(\boldsymbol{w}) = \frac{1}{n} \sum_{i=1}^n \sum_{j=1}^c P_{i,j} \log p(j|\boldsymbol{\xi}_i; \boldsymbol{w})$$

Evidently, \boldsymbol{w}_* is a minimizer of $\mathcal{G}(\boldsymbol{w})$. Similar to the last Section, we assume $\mathcal{G}(\boldsymbol{w})$ is L smooth and γ -PL function.

A straightforward approach for optimizing $\mathcal{G}(\mathbf{w})$ is, at each iteration t , sample a node i_t from the network, and compute the stochastic gradient as

$$\mathbf{g}_t = y_{i_t} \nabla_{\boldsymbol{\theta}} \log p(y_{i_t} | \boldsymbol{\xi}_{i_t}; \boldsymbol{\theta}_t)$$

and update the solution as

$$\mathbf{w}_{t+1} = \mathbf{w}_t - \eta \mathbf{g}_t$$

Following the same analysis from the last Section, we have

$$\mathbb{E} [\mathcal{G}(\mathbf{w}_{n+1}) - \mathcal{G}(\mathbf{w}_*)] \leq O\left(\frac{\log n}{n\gamma}\right)$$

and

$$\frac{1}{n} \sum_{i=1}^n \mathbb{E} \left[\sum_{j=1}^c |p(j|\boldsymbol{\xi}_i; \mathbf{w}_{n+1}) - P_{i,j}|^2 \right] \leq O\left(\sqrt{\frac{\log n}{n\gamma}}\right)$$

Here, we propose a different version of SGD, with the aim to reduce the impact of variance due to the random sample of class label y_i . We divide optimization into two phase. In the first phase, we will optimize \mathbf{w} with respect to the following objective function

$$\widehat{\mathcal{G}}(\mathbf{w}) = \frac{1}{n} \sum_{i=1}^n \sum_{j=1}^c \underbrace{\left(\frac{1}{|\mathcal{N}(i)|} \sum_{k \in \mathcal{N}(i)} q(j|\boldsymbol{\xi}_k; \boldsymbol{\theta}_1) \right)}_{:= \widehat{P}_{i,j}} \log p(j|\boldsymbol{\xi}_i; \mathbf{w})$$

In the second phase, we will run the SGD optimization that mixes stochastic gradient with the gradient of $\widehat{\mathcal{G}}(\mathbf{w})$, i.e. optimizes the objective $\lambda \widehat{\mathcal{G}}(\mathbf{w}) + (1 - \lambda) \mathcal{G}(\mathbf{w})$.

Phase I. In Phase I, we will update the solution by

$$\mathbf{w}_{t+1} = \mathbf{w}_t - \eta \nabla \widehat{\mathcal{G}}(\mathbf{w}_t)$$

Using the standard analysis, we have

$$\begin{aligned} & \mathbb{E}[\mathcal{G}(\mathbf{w}_{t+1}) - \mathcal{G}(\mathbf{w}_t)] \\ & \leq -\eta \mathbb{E} \left[\langle \nabla \mathcal{G}(\mathbf{w}_t), \widehat{\mathcal{G}}(\mathbf{w}_t) \rangle \right] + \frac{\eta^2 L}{2} \|\nabla \widehat{\mathcal{G}}(\mathbf{w}_t)\|^2 \\ & = -\frac{\eta}{2} \mathbb{E}[\|\nabla \mathcal{G}(\mathbf{w}_t)\|^2] - \frac{\eta}{2} (1 - \eta L) \mathbb{E}[\|\nabla \widehat{\mathcal{G}}(\mathbf{w}_t)\|^2] + \frac{\eta}{2} \mathbb{E}[\|\nabla \mathcal{G}(\mathbf{w}_t) - \nabla \widehat{\mathcal{G}}(\mathbf{w}_t)\|^2] \end{aligned}$$

Since

$$\begin{aligned} & \mathbb{E} \left[\|\nabla \mathcal{G}(\mathbf{w}_t) - \nabla \widehat{\mathcal{G}}(\mathbf{w}_t)\|^2 \right] \\ & = \mathbb{E} \left\| \frac{1}{n} \sum_{i=1}^n \sum_{j=1}^c (P_{i,j} - \widehat{P}_{i,j}) \nabla \log p(j|\boldsymbol{\xi}_i; \mathbf{w}_t) \right\|^2 \leq \frac{G^2}{n^2} \mathbb{E} \left\| \sum_{i=1}^n \mathbf{P}_i - \widehat{\mathbf{P}}_i \right\|^2 \leq \frac{CG^2 \log n}{n\gamma} \end{aligned}$$

and by further assuming $\eta L \leq 1$, we have

$$\mathbb{E}[\mathcal{G}(\mathbf{w}_{t+1}) - \mathcal{G}(\mathbf{w}_t)] \leq -\frac{\eta}{2} \mathbb{E}[\|\nabla \mathcal{G}(\mathbf{w}_t)\|^2] + \frac{\eta CG^2 \log n}{n\gamma}$$

or

$$\mathbb{E}[\mathcal{G}(\mathbf{w}_{t+1}) - \mathcal{G}(\mathbf{w}_*)] \leq (1 - \eta\gamma) \mathbb{E}[\mathcal{G}(\mathbf{w}_t) - \mathcal{G}(\mathbf{w}_*)] + \frac{\eta CG^2 \log n}{n\gamma}$$

By taking the telescope sum, we have

$$\mathbb{E}[\mathcal{G}(\mathbf{w}_{t+1}) - \mathcal{G}(\mathbf{w}_*)] \leq \exp(-\eta\gamma t) (\mathcal{G}(\mathbf{w}_0) - \mathcal{G}(\mathbf{w}_*)) + \frac{CG^2 \log n}{n\gamma}$$

By choosing step size $\eta = 1/L$, and setting t as

$$t = \frac{L}{\gamma} \log \frac{n\gamma(\mathcal{G}(\mathbf{w}_0) - \mathcal{G}(\mathbf{w}_*))}{CG^2 \log n}$$

we obtain the solution \mathbf{w}' with guarantee

$$\mathbb{E}[\mathcal{G}(\mathbf{w}') - \mathcal{G}(\mathbf{w}_*)] \leq \frac{2CG^2 \log n}{n\gamma}$$

Phase II. In the second phase, we use \mathbf{w}' as the initial solution for \mathbf{w} , and ran a SGD. At each iteration t , we randomly sample a node i_t from the graph, compute the gradient as

$$\mathbf{g}_t = (1 - \lambda)y_{i_t} \nabla \log p(y_{i_t}|x_{i_t}; \mathbf{w}_t) + \lambda \nabla \widehat{\mathcal{G}}(\mathbf{w}_t)$$

and update the solution as

$$\mathbf{w}_{t+1} = \mathbf{w}_t - \eta \mathbf{g}_t$$

Following the analysis from the last section, we have

$$\begin{aligned} & \mathbb{E}[\mathcal{G}(\mathbf{w}_{t+1}) - \mathcal{G}(\mathbf{w})] \\ & \leq -\eta \mathbb{E} \left[\langle \nabla \mathcal{G}(\mathbf{w}_t), (1 - \lambda) \nabla \mathcal{G}(\mathbf{w}_t) + \lambda \widehat{\mathcal{G}}(\mathbf{w}_t) \rangle \right] + \frac{\eta^2 L}{2} \mathbb{E} \left[\|\lambda \nabla \widehat{\mathcal{G}}(\mathbf{w}_t) + (1 - \lambda) \nabla \mathcal{G}(\mathbf{w}_t)\|^2 \right] + \frac{\eta^2 \eta^2 G^2 L}{2} \\ & \leq -\frac{\eta}{2} \mathbb{E} \left[\|\nabla \mathcal{G}(\mathbf{w}_t)\|^2 \right] - \frac{\eta}{2} (1 - \eta L) \mathbb{E} \left[\|\lambda \nabla \widehat{\mathcal{G}}(\mathbf{w}_t) + (1 - \lambda) \nabla \mathcal{G}(\mathbf{w}_t)\|^2 \right] + \frac{\eta \lambda^2}{2} \mathbb{E} \left[\|\nabla \mathcal{G}(\mathbf{w}_t) - \nabla \widehat{\mathcal{G}}(\mathbf{w}_t)\|^2 \right] \\ & \quad + \frac{(1 - \lambda)^2 \eta^2 G^2 L}{2} \end{aligned}$$

By choosing $\eta \leq 1/L$, we have

$$\mathbb{E}[\mathcal{G}(\mathbf{w}_{t+1}) - \mathcal{G}(\mathbf{w}_t)] \leq -\frac{\eta}{2} \mathbb{E} \left[\|\nabla \mathcal{G}(\mathbf{w}_t)\|^2 \right] + \frac{(1 - \lambda)^2 \eta^2 G^2 L}{2} + \frac{\eta \lambda^2}{2} \mathbb{E} \left[\|\mathcal{G}(\mathbf{w}_t) - \widehat{\mathcal{G}}(\mathbf{w}_t)\|^2 \right]$$

$$\begin{aligned} & \|\nabla \mathcal{G}(\mathbf{w}_t) - \nabla \widehat{\mathcal{G}}(\mathbf{w}_t)\|^2 \\ & = \left\| \frac{1}{n} \sum_{i=1}^n \sum_{j=1}^c (P_{i,j} - \widehat{P}_{i,j}) \nabla \log p(j|\boldsymbol{\xi}_i; \mathbf{w}_t) \right\|^2 \leq \frac{G^2}{n^2} \left| \sum_{i=1}^n \|\mathbf{P}_i - \widehat{\mathbf{P}}_i\|_1 \right|^2 \leq \frac{CG^2 \log n}{n\gamma} \end{aligned}$$

we have

$$\begin{aligned} & \mathbb{E}[\mathcal{G}(\mathbf{w}_{t+1}) - \mathcal{G}(\mathbf{w}_t)] \\ & \leq -\frac{\eta}{2} \mathbb{E}[\|\nabla \mathcal{G}(\mathbf{w}_t)\|^2] + \frac{(1 - \lambda)^2 \eta^2 G^2 L}{2} + \frac{\eta CG^2 \lambda^2 \log n}{n\gamma} \end{aligned}$$

Using the standard analysis, we have

$$\mathbb{E}[\mathcal{G}(\mathbf{w}_{t+1}) - \mathcal{G}(\mathbf{w}_*)] \leq \exp(-\eta\gamma t) (\mathcal{G}(\mathbf{w}') - \mathcal{G}(\mathbf{w}_*)) + \frac{CG^2 \lambda^2 \log n}{n\gamma} + \frac{(1 - \lambda)^2 \eta G^2 L}{2}$$

By minimizing over λ , we have

$$\begin{aligned} \mathbb{E}[\mathcal{G}(\mathbf{w}_{t+1}) - \mathcal{G}(\mathbf{w}_*)] & \leq \exp(-\eta\gamma t) (\mathcal{G}(\mathbf{w}') - \mathcal{G}(\mathbf{w}_*)) + G^2 \sqrt{\frac{CL\eta \log n}{2n\gamma}} \\ & \leq \frac{2CG^2 \log n}{n\gamma} \exp(-\eta\gamma t) + G^2 \sqrt{\frac{CL\eta \log n}{2n\gamma}} \end{aligned}$$

With $t = n$ and choosing

$$\eta = O\left(\frac{\log \log n}{n\gamma}\right)$$

we have

$$\mathbb{E}[\mathcal{G}(\mathbf{w}_{n+1}) - \mathcal{G}(\mathbf{w}_*)] \leq O\left(\frac{1}{n\gamma} \sqrt{\log n \log \log n}\right)$$

Comparing the naive approach where we simply train over class assignment y_i , we are able to reduce the error by a factor of $\sqrt{\log n / \log \log n}$. \square

G FURTHER RELATED WORK

Methods for Homophily and Heterophily. Many methods have been adapted to work both in homophilous and heterophilous regimes. H2GCN (Zhu et al., 2020) is one of the first methods shown to work in both kinds of datasets. RAW-GNN (Jin et al., 2022a) is a random-walk-based GCN that exploits both homophily and heterophily by doing random walks and aggregations in two ways: breadth-first for homophily and depth-first for heterophily. CPGNN (Zhu et al., 2021) is a GCN-based architecture that uses a compatibility matrix for modeling the heterophily or homophily level in the graph, which can be learned in an end-to-end fashion, enabling it to go beyond the assumption of strong homophily. GPR-GNN (Chien et al., 2020) addresses feature over-smoothing and homophily/heterophily by combining GNNs with Generalized PageRank techniques, where each step of feature propagation is associated with a learnable weight. The amplitudes of the weights trade off the degree of smoothing of node features and the aggregation power of topological features. However, all the above methods suffer from the same scalability issues that GCNs have.

Regarding scalable methods for both homophily and heterophily, the FSGNN (Maurya et al., 2021) method is closely related to our work. It relies on using propagations that are separate from the training (similar to SIGN) and uses separate (higher-order) feature propagations for homophily and heterophily. In contrast, our one-hop method relies on different components to address homophily and heterophily. Furthermore, FSGNN components can be added to our method, together with the ego features, the PEs, and the propagations, and thus their work can also be seen as complementary to ours. CLP (Zhong et al., 2022) combines a shallow (base) predictor model with a modified Label Propagation that works both in homophily and heterophily by using a class compatibility matrix (similarly to CPGNN) for the Label Propagation step. Our method is fundamentally different; however, incorporating a compatibility matrix for the propagation stage constitutes interesting future work.

Positional Embeddings. Following up on the recent success of LINKX in classifying nodes in heterophilous settings based partially on the *position* of each node (adjacency embedding), a series of methods have been suggested for incorporating positional embeddings on graph methods (Kim et al., 2022; Dwivedi et al., 2021). More specifically, (Dwivedi et al., 2021) proposes the MLPGNN-LSPE architecture, which can simultaneously learn both structural and positional embeddings for nodes, whereas (Kim et al., 2022) proposes TokenGT, which treats all nodes and edges as independent tokens, augments them with positional embeddings – eigenvectors of the normalized Laplacian of the graph ignoring edge directions – and then feeds them to a Transformer model. However, creating positional embeddings that require the factorization of the Laplacian matrix is impractical for large-scale graphs. For this reason, various methods have been proposed for embedding nodes in a graph in a scalable manner, such as TransE (Bordes et al., 2013), DistMult (Yang et al., 2014)⁷. The recent development of Pytorch-Biggraph (Lerer et al., 2019) allows training KGEs large heterogeneous graphs (El-Kishky et al., 2022).

⁷For more such methods see (Lerer et al., 2019) and the references therein.